Fluorescence signaling of ligand binding and assembly in metal-chelating lipid membranes

KM Maloney, DR Shnek[†], DY Sasaki[‡] and FH Arnold[*]

Background: Chemical information is sometimes transmitted across cell membranes by ligand-induced assembly of receptors. We have previously designed a series of lipids with metal-chelating headgroups that can serve as general receptors for proteins containing accessible histidines. Such lipids can also be derivatized with pyrene, a fluorescent probe that has a different emission maximum when it is aggregated (excimer fluorescence) from that seen for the monomer. We set out to examine whether lipids of this kind would produce a signal in response to ligand binding.

Results: A model ligand, poly-L-histidine (poly(His)), bound specifically to pyrene-labeled Cu(II)-iminodiacetate lipid (Cu-PSIDA) within a membrane matrix. Binding of poly(His) induces the redistribution of Cu-PSIDA, so that it forms pyrene-rich domains that are detectable by the increased ratio of excimer to monomer fluorescence. Using rhodamine-labeled poly(His), we have shown that the receptor lipid domains correspond to poly(His)-rich domains below the lipid interface.

Conclusions: The Cu-PSIDA receptor signals binding of the macromolecular ligand through its excimer fluorescence and allows the resulting domains formed by ligand assembly to be imaged. Fluorescent Cu-PSIDA can thus serve as an optical reporter of ligand-induced lipid reorganization.

Address: Division of Chemistry and Chemical Engineering 210-41, California Institute of Technology, Pasadena, CA 91125, USA. Phone: (818) 395-4162; Fax: (818) 568-8743; Email: frances@macpost.caltech.edu

Present addresses: [†]Eli Lilly & Co., Lilly Corporate Center, Indianapolis, IN 46285, USA and [‡]Sandia National Laboratory, Albuquerque, NM 87185-1407, USA.

*Corresponding author.

Key words: artificial cells, copper, iminodiacetate, lipid organization, poly-L-(histidine), pyrene excimer

Received: **22 Jan 1996**
Revisions requested: **6 Feb 1996**
Revisions received: **28 Feb 1996**
Accepted: **4 March 1996**

Chemistry & Biology March 1996, **3**:185–192

 ISSN 1074-5521

Introduction

Biological membranes have inspired new approaches to chemical sensing and signaling [1,2], to the preparation of functional molecular devices [3] and to the control of the architecture of crystalline organic and inorganic materials grown from patterned surfaces [4]. Several features are required for membrane-based materials to fulfill their potential, including precise control of membrane surface architectures and the interactions between biomolecules and the surface, and mechanisms for generating signals. Lipid membrane systems are particularly attractive for these kinds of applications, because they spontaneously self-organize to form a range of well-defined structures of varied size that can serve as scaffolds for further molecular recognition and binding events. Also, the components of lipid membranes are mobile enough to allow lateral lipid reorganization, so that external ligands can be further organized after they are bound to the membrane. Thus, lipid membranes can assist the assembly of bound ligands into interesting superstructures. For example, organic and inorganic crystals can be nucleated and grown on the membrane surface [4], and proteins can self-assemble into domains which may also be crystalline in two dimensions (see [5] for a recent review). Conversely, external ligands can induce microstructural changes in the membrane, altering the distribution of individual components of the lipid matrix and leading to lateral lipid phase separation [6–8] or to the formation of functional assemblies that can transmit chemical information across the cell membrane [9,10].

We have attempted to construct simple, robust non-biological systems that reproduce some of the important features of biological targeting and self-assembly in synthetic lipid membranes. We have therefore designed a series of lipids with iminodiacetate (IDA) headgroups to serve as general synthetic receptors, targeting biomolecules to lipid monolayers and bilayers [11–13]. Ligands (e.g., protein) form a ternary-coordination complex with a metal ion chelated by the IDA headgroup. IDA chelates Cu(II) with a K_a near 10^{11} M^{-1} [14]. At neutral pH, histidine residues on protein surfaces can coordinate to IDA-bound Cu(II) ($K_a \approx 10^{3.5}$ M^{-1}, [15]); other amino acid side chains do not exhibit significant affinity for the IDA-bound metal ion at pH 7. A wide variety of ligands can bind to Cu(II)- and Ni(II)-chelating lipid membranes, including native proteins with surface-accessible histidines [12,13], genetically engineered hexahistidine fusion proteins [11,16] and synthetic histidine-containing peptides [17].

In addition to acting as a specific membrane-resident affinity ligand, an IDA-lipid derivatized with pyrene in the aliphatic lipid tail (PSIDA, Fig. 1) can report on lateral reorganization in the lipid membrane induced by ligand

binding, since aggregated pyrene-labeled lipids can form more excimers than monomeric pyrene lipid. The increased excimer formation leads to a strong emission at the longer (excimer) wavelength. The generation of an optical signal upon ligand binding to PSIDA is useful for sensor applications [18] as well as for observing the membrane and/or ligand reorganization that accompanies binding and assembly. Pyrene-labeled lipids have been widely used to study protein–membrane interactions [19–23]. The ratio of pyrene excimer to monomer fluorescence intensities (the E/M ratio) is directly related to intermolecular pyrene-lipid collisional rates and local pyrene concentration [7,24,25]. Thus, changes in the diffusivity and distribution of the general lipid receptor are revealed in the pyrene fluorescence emission.

Figure 1 shows the emission spectra of PSIDA (5 mol %) in two different lipid bilayer systems: 1-stearoyl-2-oleoyl-sn-glycero-3-phosphocholine (SOPC) and 1,2-distearoyl-sn-glycero-3-phosphocholine (DSPC). PSIDA monomer (377 nm) and excimer (477 nm) emission intensities differ markedly in these bilayers, one of which (SOPC) is fluid and the other (DSPC) is in a gel state at room temperature. The difference in the physical state of the bilayer has a significant effect on the PSIDA E/M ratio: the fluid-like PSIDA mixes more readily in SOPC bilayers and exhibits a much smaller E/M ratio than it does in a DSPC matrix. We previously showed that divalent transition metals could induce a comparably large decrease in the PSIDA E/M ratio in a DSPC lipid bilayer [18]. This is thought to be due to metal-induced de-aggregation of the PSIDA lipid, leading to its lateral redistribution.

Figure 1

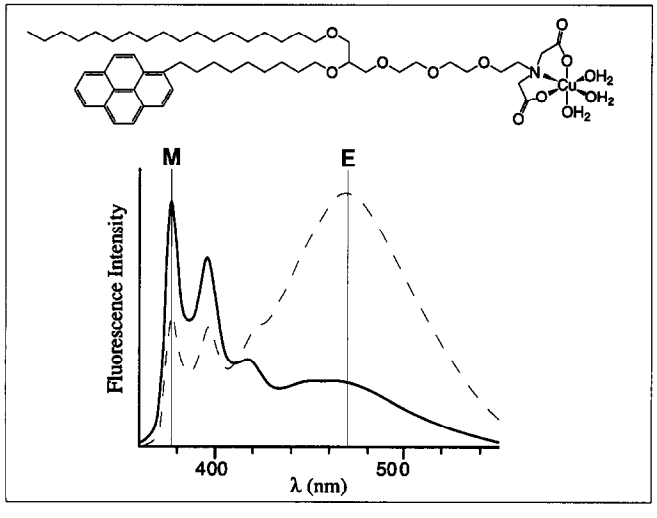

Chemical structure and fluorescence spectra of PSIDA in sonicated bilayered vesicles. Fluorescence emission spectra of binary mixed PSIDA:SOPC (5:95; solid line) and PSIDA:DSPC (5:95; broken line) vesicles are shown. M, monomer fluorescence; E, excimer fluorescence. Excitation wavelength is 337 nm.

Here we show that the receptor PSIDA lipid with bound copper(II) can report on ligand binding, as a result of the ability of the ligand to redistribute the receptor in the membrane. In a process analogous to natural membrane receptor assembly and signal transduction [9,10], binding of an external multivalent ligand localizes the PSIDA receptor lipids, resulting in a strong excimer signal. Using a monolayer of lipids as a model membrane and fluorescence microscopy to monitor pyrene excimer fluorescence, we can visualize how the binding of a macromolecule rich in metal-coordinating histidine ligands alters the lateral distribution of Cu-PSIDA receptor lipids, creating pyrene-enriched domains. By labeling the ligand, poly-L-histidine (poly(His)), with a second fluorophore (rhodamine), we can also show that the ligand-induced lipid domains correspond to the poly(His) domains that form beneath the lipid monolayer. Thus, the pyrene-labeled lipid can produce a signal on binding of the metal-coordinating macromolecular ligand. We can therefore image the resulting ligand domains by way of the complementary receptor lipid domains formed within the membrane.

Results

Poly(His)–Cu-PSIDA interactions in monolayers at the air–buffer interface

Our objectives in investigating the interactions between poly(His) and Cu-PSIDA in lipid monolayers at the air–buffer interface were two-fold. First, we wished to demonstrate that the Cu-PSIDA receptor lipid could specifically target a histidine-rich ligand to those regions of a membrane surface that contain the receptor lipid. Second, we wanted to investigate whether poly(His) binding could induce reorganization of the receptor lipid in an initially well-mixed membrane system. The latter result would tell us whether the fluorescent PSIDA lipid could be used to signal ligand binding and assembly.

To address whether ligand is specifically targeted to domains containing Cu-PSIDA, we prepared a lipid monolayer consisting of a Cu-PSIDA-rich phase in coexistence with a non-binding lipid phase from an equimolar mixture of Cu-PSIDA and 1,2-dibehenoyl-sn-glycero-3-phosphocholine (DBPC). Phase separation in this system is based largely on the difference in the hydrophobic chain lengths of PSIDA (18 carbons) and DBPC (22 carbons). At a surface pressure of 27 mN m^{-1}, fluorescence microscopy reveals dark regions in the monolayer where PSIDA is excluded (Fig. 2a). Figure 2a was imaged using an emission filter selective for pyrene excimer fluorescence (λ_{em} = 470 ± 25 nm). The dark zones consist mainly of DBPC, as the shorter, bulkier Cu-PSIDA lipid prefers not to pack in condensed monolayer phases. Strong PSIDA excimer fluorescence illuminates the bright regions, showing that the receptor lipid has separated into domains enriched in Cu-PSIDA. Addition of poly(His) labeled with a second

fluorophore, rhodamine (rhodamine-poly(His)), to the 1:1 Cu-PSIDA:DBPC monolayer subphase led to polymer adsorption to the monolayer interface. A micrograph (Fig. 2b) of the same phase-separated Cu-PSIDA:DBPC monolayer depicted in Figure 2a, taken with a fluorescence filter specific for rhodamine emission ($\lambda_{em} > 590$ nm), shows rhodamine fluorescence corresponding to the regions that display PSIDA excimer fluorescence. Little to no rhodamine fluorescence is observed from the DBPC domain, indicating that poly(His) is targeted to the regions rich in Cu-PSIDA and not to the DBPC domains. Control experiments performed with 100 μM EDTA in the monolayer subphase to sequester the metal ions showed that rhodamine-poly(His) binding to PSIDA:DBPC mixed monolayers requires Cu(II).

Figure 2

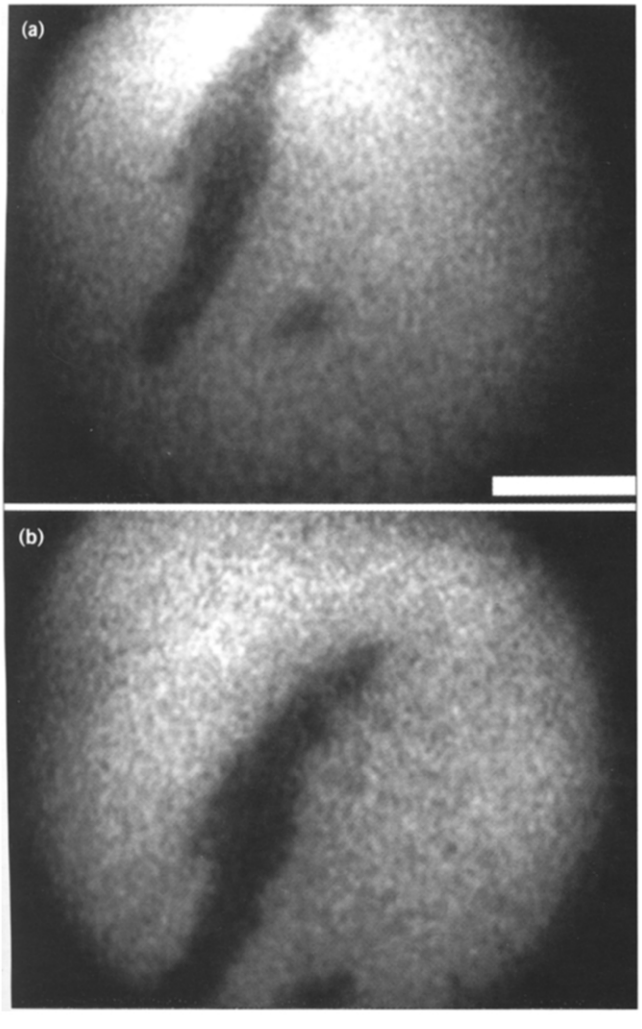

Phase separation in Cu-PSIDA:DBPC membranes can be used to show the specificity of poly(His) binding. Fluorescence micrographs of Cu-PSIDA:DBPC (1:1) mixed monolayers at the N_2–buffer interface, visualized using **(a)** pyrene excimer emission or **(b)** rhodamine emission filters. Experimental conditions: surface pressure = 27 mN m^{-1}, room temperature (RT), subphase buffer is 100 mM NaCl, 20 mM MOPS, pH 7.5, rhodamine-poly(His) = 250 nM. Scale bar in (a) is 100 μm.

The interactions of poly(His) with initially well-mixed monolayers containing PSIDA and a non-binding matrix lipid were investigated as a model membrane signal-generating system. From previous monolayer mixing and fluorescence microscopy studies [11], binary Cu-PSIDA:SOPC monolayers are known not to phase-separate at room temperature. Poly(His) was added to the aqueous subphase of a Cu-PSIDA:SOPC (5 mol %:95 mol %) monolayer, and changes in the fluorescent properties of Cu-PSIDA were monitored using fluorescence microscopy to determine whether PSIDA could signal interfacial polymer binding through enhanced PSIDA excimer fluorescence emission. In the absence of poly(His), the Cu-PSIDA:SOPC monolayer exhibits homogeneous PSIDA fluorescence and is free of apparent membrane microstructures (to a lateral resolution of ~5 μm). When poly(His) is injected beneath the monolayer at constant surface pressure (25 mN m^{-1}), changes in the lateral distribution of PSIDA fluorescence are apparent. A pair of fluorescence micrographs of a Cu-PSIDA:SOPC monolayer in the presence of poly(His) is shown in Figure 3. Figure 3a, imaged using the filter selective for pyrene excimer fluorescence, shows a membrane domain displaying intense excimer fluorescence surrounded by weaker excimer signal. The same monolayer field of view was then re-imaged using an emission filter specific for pyrene monomer fluorescence ($\lambda_{em} = 402 \pm 15$ nm; Fig. 3b). The bright excimer domain in Figure 3a is barely observable in Figure 3b; the monomer signal is weak throughout the field of view. The excimer domains routinely formed by poly(His) under these conditions are circular structures 30–40 μm in diameter.

Control experiments were performed to confirm that formation of the monolayer microstructures depicted in Figure 3 is mediated by Cu(II) and PSIDA. When poly(His) was added to Cu(II)-free PSIDA:SOPC monolayer subphases (with EDTA present to chelate residual metal ions), the bright excimer regions observed in Figure 3a were absent. Moreover, when rhodamine-poly(His) was added to the subphase of a pure SOPC monolayer in the presence of Cu(II), the fluorescent polymer did not assemble into domains at the interface.

These experiments were conducted at fairly high monolayer surface pressure (25 mN m^{-1}) to block non-specific poly(His) insertion into the monolayer. Within the observation times used to visualize poly(His)-induced PSIDA excimer domain formation (typically 1–4 h), the mean molecular areas did not change significantly. Thus, formation of the PSIDA excimer domains (Fig. 3a) is not due to non-specific insertion of the polymer into the monolayer.

Figure 3

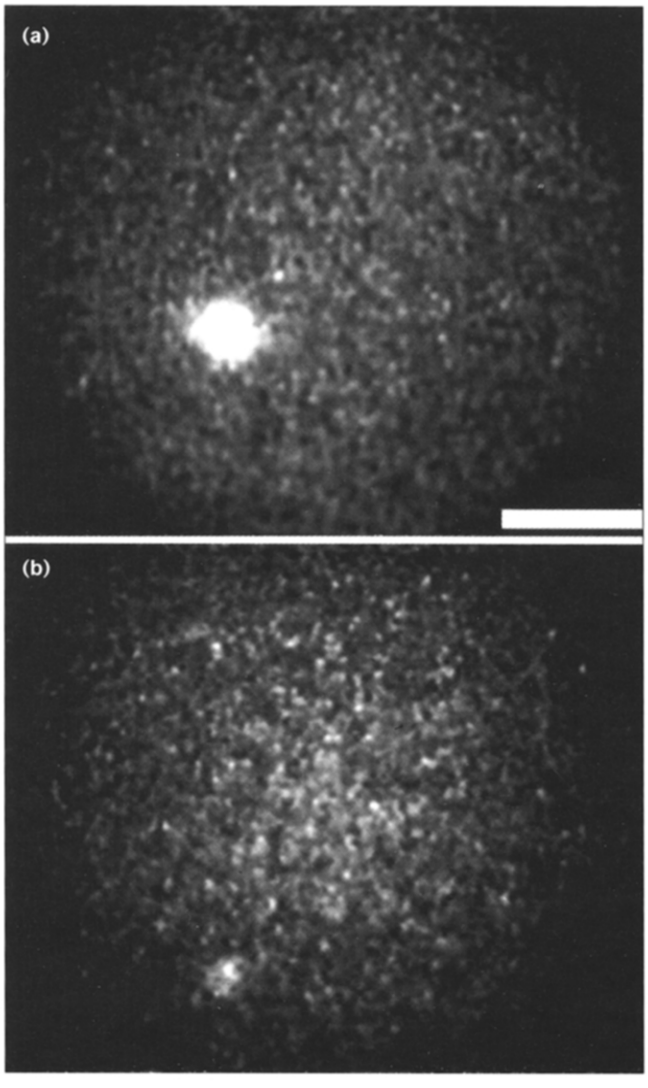

Poly(His) causes changes in the lateral distribution of Cu-PSIDA in the membrane. Fluorescence micrographs of Cu-PSIDA:SOPC (5:95) mixed monolayers at the N_2–buffer interface, visualized using **(a)** pyrene excimer and **(b)** pyrene monomer fluorescence emission filters. Experimental conditions: surface pressure = 25 mN m^{-1}, RT, subphase buffer is 100 mM NaCl, 20 mM MOPS, pH 7.5, poly(His) = 500 nM. Scale bar in (a) is 100 μm.

The fluorescence micrographs in Figure 3 strongly suggest that poly(His) is bound beneath the excimer-rich monolayer regions and that the multiple His ligands available on the polymer allow it to crosslink PSIDA lipids. To verify the location of the polymer, rhodamine-poly(His) binding experiments analogous to those discussed in Figure 3 were conducted (Fig. 4a). The formation of excimer-rich regions observed with unlabeled poly(His) were also apparent with rhodamine-poly(His); thus the fluorescent label does not affect the polymer's ability to induce excimer domain formation. Re-imaging the excimer domain in Figure 4a using a filter specific for rhodamine emission (λ_{em} > 590 nm) gave the image shown in Figure 4b. The fact that the excimer domain in Figure 4a also fluoresces when observed using rhodamine-specific fluorescence filters confirms that rhodamine-poly(His) binds the monolayer in those regions exhibiting intense excimer lipid fluorescence. Figures 3 and 4, together with the control experiments, show that metal-mediated poly(His) interactions with the mixed Cu-PSIDA:SOPC monolayer lead to PSIDA domain formation, and that the ligand is concentrated beneath these regions.

Poly(His)–Cu-PSIDA interactions in bilayer vesicles

To determine whether the ligand-induced changes in PSIDA fluorescence could also be observed

Figure 4

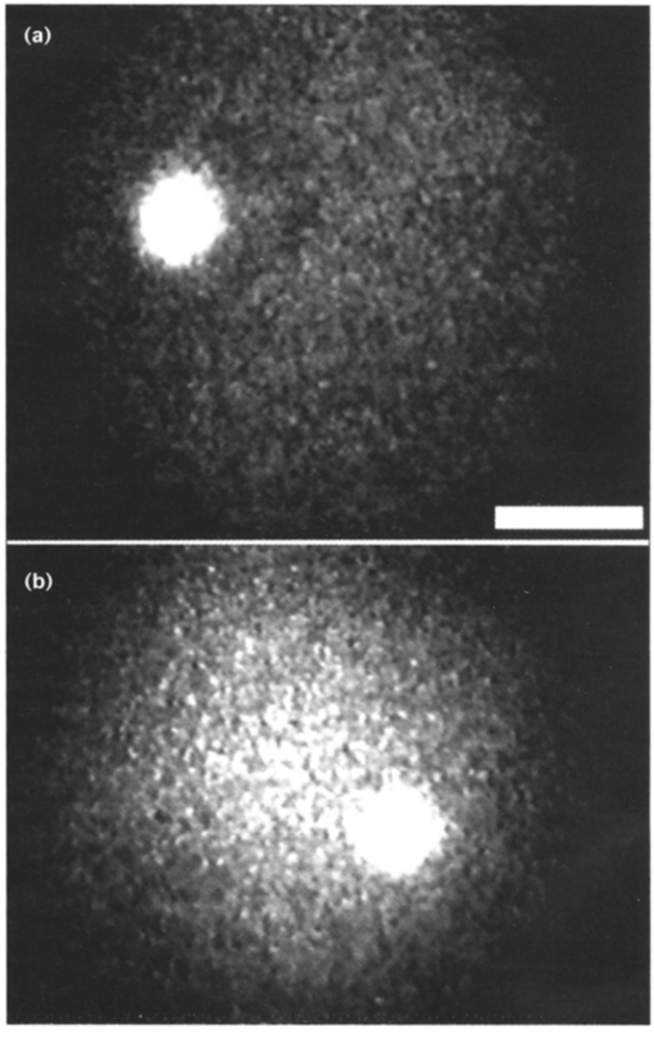

Poly(His) is localized to the regions of the membrane that show excimer fluorescence. Fluorescence micrographs of Cu-PSIDA:SOPC (5:95) mixed monolayers at the N2–buffer interface. Images were visualized using **(a)** pyrene excitation-pyrene excimer emission and **(b)** rhodamine excitation-rhodamine emission fluorescence emission filters, respectively. Experimental conditions as for Fig. 3. Scale bar in (a) is 100 μm.

spectroscopically in bilayer membranes, we examined the interactions of poly(His) with Cu-PSIDA-doped vesicles. Metal binding has previously been shown to decrease the PSIDA E/M ratio in vesicles containing DSPC as the matrix lipid [18]; we believe that Cu-PSIDA (5 %) is well mixed in the DSPC matrix (95 %). We therefore examined the changes in the E/M ratio (Δ(E/M)) of the Cu-PSIDA in DSPC vesicles as a function of added poly(His) (Fig. 5). We define Δ(E/M) as the difference between the E/M ratio at a particular poly(His) concentration and the ratio seen in the absence of poly(His).

Poly(His) interactions with Cu-PSIDA mixed vesicles caused the E/M ratio to increase by as much as 60 %, with a plateau at ~0.5 μM poly(His) (Fig. 5, ▼). Control experiments conducted in the absence of Cu(II) revealed that the PSIDA E/M ratio is essentially unaffected by the presence of poly(His) when copper is not present (Fig. 5, ○). As in the case of the PSIDA-based metal ion sensor [18], E/M ratios in binary Cu-PSIDA:DSPC vesicles are sensitive to and signal the presence of bound ligand.

To probe how the matrix lipid affects Cu-PSIDA E/M ratios in the presence of poly(His), we also monitored changes in Cu-PSIDA Δ(E/M) in Cu-PSIDA:SOPC (5:95) vesicles. Over an equivalent poly(His) concentration range, the overall change in the Cu-PSIDA:SOPC vesicle Δ(E/M) was significant, but not as large as that seen in the Cu-PSIDA:DSPC system (data not shown).

Figure 5

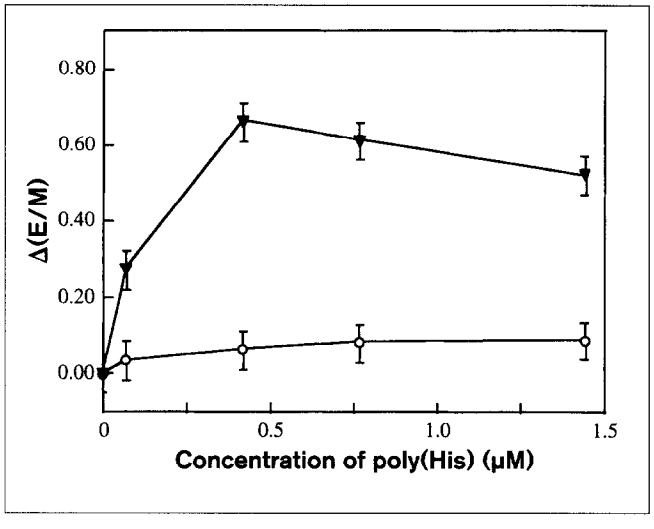

Cu-PSIDA lipids in lipid bilayers can signal ligand binding. Change in Cu-PSIDA fluorescence due to poly(His) binding to mixed Cu-PSIDA:DSPC (5:95; mol:mol) vesicles (▼). PSIDA:DSPC mixed vesicles (19 μM total lipid) were in 20 mM MOPS, 100 mM NaCl, pH 7.5 at 25 °C. Control experiments (○) were conducted in the absence of $CuCl_2$. $\Delta(E/M) = (E/M)_{poly(His)} - (E/M)_0$. For Cu-PSIDA:DSPC vesicles, $(E/M)_0 = 0.26$. For vesicles prepared in the absence of metal ions, $(E/M)_0 = 0.43$.

Moreover, the dependence of Cu-PSIDA Δ(E/M) on added poly(His) concentration was more complex than the saturation-type behavior displayed in Figure 5. Further investigations will be required to elucidate the role of the matrix lipid in ligand binding and assembly in these Cu-PSIDA-containing vesicles.

Discussion

To mimic the features of biological membranes that are important for sensors and template (surface pattern)-assisted crystal growth applications, we require robust synthetic systems that show: 1) specific ligand binding, 2) ligand-induced receptor reorganization, 3) ligand assembly at the membrane interface, and 4) signal generation in response to ligand binding. Specific interfacial binding and orientation of metal-coordinating ligands can be effected using the IDA lipids complexed to Cu(II) and Ni(II) [12]. Although the binding constant for a single histidine–Cu-PSIDA interaction is not strong compared to many interactions seen in biological systems, several simultaneous interactions can lead to binding affinities comparable to antigen–antibody interactions [11]. Many important biological structures — protein assemblies, viruses and even cells — are rich in metal-coordinating functional groups. The unique spatial distributions of these groups on the surfaces of biological structures may provide a mechanism for their recognition [26]. Alternatively, these functional group patterns, especially in ordered arrays such as two-dimensional crystals, could serve as templates for the growth of interesting organic or inorganic structures.

The exploitation of multipoint ligand–membrane interactions is an important feature of the current effort to control surface pattern formation and signal ligand binding in membrane-mimetic systems. Upon addition of a multi-histidine ligand that can bind to several Cu-PSIDA lipids simultaneously, the PSIDA will reorganize in the matrix lipid to complement the pattern of histidines presented by the bound ligand (Fig. 6). The E/M behavior of the pyrene-labeled IDA lipid should then change, signaling the fact that the ligand has bound to the membrane.

The extent to which bound ligands can assemble into superstructures and induce lipid reorganization clearly depends on the nature of the lipids as well as that of the ligand. The intrinsic pattern of the phase-separated Cu-PSIDA:DBPC lipid monolayer, for example, dictated the resulting pattern of adsorbed ligand (Fig. 2). Similar results have been described by Tampé and co-workers [17], who studied peptide binding to a phase-separated monolayer containing a Ni(II)-nitrilotriacetate (NTA)-lipid. But when it is possible for the receptor lipids to redistribute within the membrane, one can use the signaling capacity of the fluorescent lipid to detect ligand binding, or ligand aggregation. Here we have shown that

Figure 6

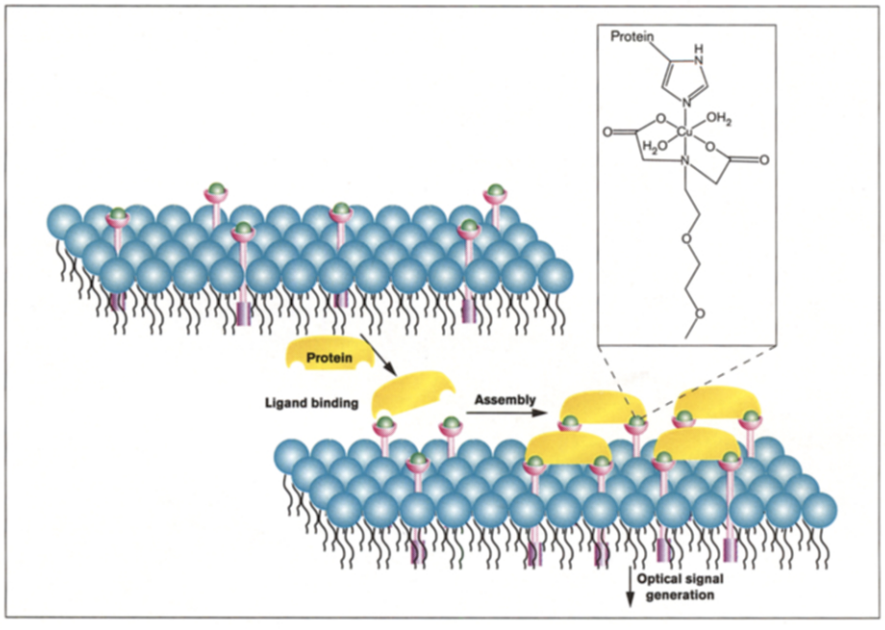

Schematic drawing of ligand binding and assembly processes on a mixed membrane containing receptor/reporter lipids (Cu-PSIDA). Multipoint ligand binding and assembly induces reorganization of pyrene reporter groups in the membrane and generation of a fluorescent (excimer) signal. When accompanied by assembly of the ligand into domains or arrays (e.g. two-dimensional crystals), ligand binding results in the formation of macroscopic membrane regions enriched in Cu-PSIDA.

poly(His) can direct the complementary assembly of metal-chelating lipids in the initially well-mixed Cu-PSIDA:SOPC monolayer. Poly(His) aggregates into domains beneath the lipid monolayer probably as a result of the high local poly(His) concentrations facilitated by surface binding and the mobility of the lipid receptor. A protein with accessible surface histidines should exhibit similar behavior if it can be concentrated at the interface to the point where protein–protein and protein–solvent interactions favor precipitation (or crystallization) [13].

The changes in the PSIDA E/M ratios in response to ligand binding should vary depending on how many available histidine residues the ligand contains, their spatial distribution, and whether the ligand tends to form superstructures. Changes in the E/M ratios could also result from altered PSIDA diffusivity in the membrane when ligand is bound. Ligands that induce lateral Cu-PSIDA aggregation would be expected to increase the E/M ratio, while those that inhibit PSIDA–PSIDA diffusional encounters would be expected to decrease it. Because biological assemblies such as viruses present unique patterns of histidine residues, it is conceivable that specific optical signals could be generated upon binding to mixed monolayers containing the fluorescent Cu-IDA receptors. Different optical (e.g., resonance energy transfer), physical (e.g. electronic), or chemical signals could be generated using lipids modified with other functional groups in place of pyrene.

Poly(His) is assembled into microscopic domains upon specific interfacial binding to the Cu-PSIDA-containing monolayer (Figs 3,4). These domains are large enough to be imaged by fluorescence microscopy. Similar behavior has been observed previously upon electrostatically-driven polymer binding to lipid membranes. The excimer fluorescence of pyrene probe molecules indicates that poly-L-lysine induces phase separation in bilayer membranes of negatively charged phospholipids [8,27]. A variety of proteins targeted to lipid monolayers also assemble into domains under appropriate conditions, forming ordered arrays and even two-dimensional crystals [5]. Where targeted ligands can be crystallized in two dimensions using metal–histidine interactions, as reported recently by this laboratory for native streptavidin [13] and by Kubalek *et al.* for histidine-tagged HIV reverse transcriptase [16], the lateral membrane receptor distribution should complement the histidine distribution in the assembled ligand domain (protein crystal), as it does for poly(His). It is thus conceivable that the general, metal-mediated, surface-monolayer targeting mechanism described here can be used in conjunction with two-dimensional protein crystallization to form specific, molecular-level surface patterns of metal complexes and extend those patterns over the macroscopic dimensions of the protein crystals (Fig. 6). The formation of these complementary receptor patterns could be exploited to generate specific signals. Alternatively, patterns fixed, for example, by crosslinking polymerization of the matrix lipids could be used as specific binding surfaces [26], as templates for crystal growth (e.g., in biomineralization), or for coupling to other components to enhance signal transduction or to prepare optoelectronic devices.

The data presented here suggest that the processes illustrated in Figure 6 can be realized in this synthetic membrane system. Figures 3 and 4 show that PSIDA can report on ligand-induced changes in lateral membrane organization through its excimer fluorescence intensity. Beginning with a well-mixed, laterally homogeneous membrane, addition of poly(His), which presumably binds multiple Cu-PSIDA lipids and which also aggregates into domains on the monolayer surface, induces the formation of regions rich in PSIDA and high in excimer fluorescence intensity. The E/M ratio of Cu-PSIDA in bilayer vesicles is also sensitive to the presence of poly(His) (Fig. 5), suggesting that lipid reorganization occurs during poly(His) binding to lipid bilayers as well.

Significance

Specific binding and assembly of external ligands by membrane surfaces underlies important cellular processes as well as efforts to produce robust, non-biological functional materials. General receptors for promoting interfacial binding in defined orientations are needed, as are physical methods to signal ligand binding and/or membrane reorganization. We have therefore designed a fluorescent chelating lipid that functions as a membrane-resident affinity receptor/reporter for ligands that bind via coordination to a lipid-bound metal ion (Cu(II)); the lipid then generates a signal using pyrene excimer fluorescence. The Cu(II)-chelating lipid can serve as a receptor for a wide range of molecules with metal-coordinating functional groups, including proteins that have surface-accessible histidine residues. Depending on the nature of the lipid matrix and the targeted ligand, synthetic membranes containing the metal-chelating lipid can promote the assembly of bound ligands, resulting in receptor reorganization and the generation of an optical signal. Other physical or chemical signals could be generated by this general approach, which mimics the general strategy of receptor assembly-mediated signal transduction in the membranes of natural cells.

This metal-chelating fluorescent lipid could be useful in several areas of biologically-inspired materials research. This robust receptor/reporter system can be used to probe ligand binding and assembly processes in synthetic monolayer and bilayer membranes. Synthetic metal-chelating membrane assemblies could be used for sensor applications, while the formation of long-range patterns of functional surface groups or reporter molecules via two-dimensional crystallization of bound ligands should be useful in the preparation of ordered materials and bioelectronic devices.

Materials and methods

Materials

3-[N-morpholino]propanesulfonic acid (MOPS) buffer (99.5 %), NaCl (99 %), $CuCl_2 \cdot H_2O$ (99.8 %), $CHCl_3$ (HPLC grade), and poly-L-histidine (M_r ~ 11 100) were purchased from Sigma (St. Louis, MO). L-α-1-Stearoyl-2-oleoyl-sn-glycero-3-phosphocholine (SOPC) and L-α-1,2-distearoyl-sn-glycero-3-phosphocholine (DSPC) were purchased from Avanti Polar Lipids (Alabaster, AL) and L-α-1,2-dibehenoyl-sn-glycero-3-phosphocholine (DBPC) was from Sigma Chemicals (St. Louis, MO). 1-stearyl-2-(9-pyrenylnonyl)-rac-glycero-3-(8-(3,6-dioxy)octyl-1-amino-N,N,diacetic acid) (PSIDA, Fig. 1) was prepared as described previously [11]. Rhodamine B-conjugated poly(His) (rhodamine-poly(His)) was prepared using the carbodiimide method of carboxylate modification [28] and purified using gel filtration chromatography (PD-10 column, Pharmacia). The fluorescent peptide conjugate displayed a maximum absorbance at 560 nm and an emission maximum at 620 nm.

Vesicle preparation

Binary mixed PSIDA:SOPC and PSIDA:DSPC vesicles were prepared by mixing appropriate amounts of stock solutions of chloroform-dissolved lipid followed by solvent evaporation. The resultant lipid film was hydrated in aqueous buffered solution at temperatures above the lipid melting temperature (T_m) and microtip sonicated (Heat Systems, Inc., Farmingdale, NY) under an Ar atmosphere for 10 min in an ice bath. Following sonication, the vesicles were centrifuged for 20 min at 14 000 rpm to remove titanium released from the sonicator microtip and then filtered through 0.2 μm Nalgene filters.

Fluorescence spectroscopy

Vesicle stock solutions (3.3 mM) were diluted for fluorescence experiments to prevent turbidity effects due to peptide-induced inter-vesicle cross linking. UV absorption of vesicle samples at 1:500 dilution showed no absorption spectra due to turbidity (300 nm). A Shimadzu RF-540 spectrofluorimeter fitted with a temperature controlled bath was used for steady-state fluorescence intensity measurements. Pyrene excitation wavelength was set at 346 nm with emission scanned from 370–550 nm (5 nm slits). Fluorescence intensities at 377 nm and 470 nm were measured to determine the E/M ratio.

Fluorescence microscopy

Fluorescence microscopy [29–31] of lipid monolayers at the air–buffer interface was conducted using a computer-controlled, double-barrier trough (LB-1000, KSV, Helsinki, Finland) placed on the stage of an inverted fluorescence microscope (Axiovert, Zeiss, AGM) as described previously [11]. Nitrogen or argon atmospheres surrounding the trough were required for PSIDA monolayer imaging because of oxygen quenching of pyrene fluorescence. PSIDA was allowed to bind metal ions prior to monolayer formation; stock PSIDA solutions were mixed with equimolar amounts of methanol-dissolved $CuCl_2$. Monolayers were compressed at a rate of 1.6 $Å^2$ per molecule min^{-1}; upon reaching 25 mN m^{-1}, surface pressure was held constant while poly(His) was injected into the monolayer subphase from behind the trough barrier. Steady-state PSIDA fluorescence intensities were obtained using a Melles Griot 03FIM026 excitation filter, Omega Optical 355DRLP dichroic mirror, 405DF40 monomer filter and 470DF35 excimer filter. Rhodamine fluorescence intensities were obtained using an Omega 560DF40 excitation filter, 600DRLP02 dichroic mirror and 630DF30 emission filter.

Acknowledgements

This research was supported by the Office of Naval Research (N00014-92-J-1178) and by a postdoctoral fellowship (1F32GM16953-01A1) to K.M.M. from the National Institute of General Medical Sciences.

References

1. Stelzle, M., Weissmuller, G. & Sackmann, E. (1993). On the application of supported bilayers as receptive layers for biosensors with electrical detection. *J. Phys. Chem.* **97**, 2974–2981.
2. Charych, D.H., Nagy, J.O., Spevak, W. & Bednarski, M.D. (1993). Direct colorimetric detection of a receptor–ligand interaction by a polymerized bilayer assembly. *Science* **261**, 585–588.

3. Samuelson, L.A., *et al.*, & Kaplan, D.L. (1992). The monomolecular organization of a photodynamic protein system through specific surface recognition of streptavidin by biotinylated Langmuir–Blodgett films. *Langmuir* **8**, 604–608.
4. Mann, S., *et al.*, & Reeves, N.J. (1993). Crystallization at inorganic–organic interfaces – biominerals and biomimetic synthesis. *Science* **261**, 1286–1292.
5. Jap, B.K., *et al.*, & Engel, A. (1992). 2D crystallization: from art to science. *Ultramicroscopy* **46**, 45–84.
6. Eklund, K.K., Vuorinen, J., Mikkola, J., Virtanen, J.A. & Kinnunen, P.K.J. (1988). Ca^{2+}-induced lateral phase-separation in phosphatidic acid/phosphatidylcholine monolayers as revealed by fluorescence microscopy. *Biochemistry* **27**, 3433–3437.
7. Galla, H.J. & Hartmann, W. (1980). Excimer forming lipids in membrane research. *Chem. Phys. Lipids.* **27**, 199–219.
8. Sackmann, E. (1978). Dynamic molecular organization in vesicles and membranes. *Ber. Bunsenges. Phys. Chem.* **82**, 891–909.
9. DeLisi, C. & Siraganian, R.P. (1979). Receptor cross-linking and histamine release: I. the quantitative dependence of basophil degranulation on the number of receptor doublets. *J. Immunol.* **122**, 2286–2292.
10. Shimohigashi, Y., Costa, T., Chen, H.-C. & Rodbard, D. (1982). Dimeric tetrapeptide enkephalins display extraordinary selectivity for δ-opiate receptors. *Nature* **297**, 333–335.
11. Ng, K., Pack, D.W., Sasaki, D.Y. & Arnold, F. H. (1995). Engineering protein–lipid interaction: targeting of histidine-tagged proteins to metal-chelating lipid monolayers. *Langmuir* **11**, 4048–4055.
12. Shnek, D.R., Pack, D.W., Sasaki, D.Y. & Arnold, F.H. (1994). Specific protein attachment to artificial membranes via coordination to lipid-bound copper (II). *Langmuir* **10**, 2382–2388.
13. Frey, W., *et al.*, & Arnold, F.H. (1996). 2-D protein crystallization via metal ion coordination by naturally occurring surface histidines. *Proc. Natl. Acad. Sci. USA*, in press.
14. Martell, A.E. & Smith, R.M. (1975). *Critical Stability Constants. (Vol. 2: Amines).* Plenum Press, New York.
15. Sinha, P.C., Saxena, V.K., Nigam, N.B. & Srivastava, M.N. (1989). Mixed ligand complexes of copper(II), nickel(II), cobalt(II), & zinc(II) with iminodiacetate as a primary ligand and imidazole as a secondary ligand. *Indian J. Chem.* **28**, 335–336.
16. Kubalek, E.W., Legrice, S.F.J. & Brown, P.O. (1994). 2-Dimensional crystallization of histidine-tagged, HIV-1 reverse-transcriptase promoted by a novel nickel-chelating lipid. *J. Struct. Biol.* **113**, 117–123.
17. Dietrich, C., Schmitt, L. & Tampé, R. (1995). Molecular organization of histidine-tagged biomolecules at self-assembled lipid interfaces using a novel class of chelator lipids. *Proc. Natl. Acad. Sci. USA* **92**, 9014–9018.
18. Sasaki, D.Y., Shnek, D.R., Pack, D.W. & Arnold, F.H. (1995). Metal-induced dispersion of lipid aggregates: a simple, selective, and sensitive fluorescent metal ion sensor. *Angew. Chem. Int. Ed. Engl.* **34**, 905–907.
19. Haverstick, D.M. & Glaser, M. (1989). Influence of proteins on the reorganization of phospholipid-bilayers into large domains. *Biophys. J.* **55**, 677–682.
20. Wiener, J.R., Pal, R., Barenholz, Y. & Wagner, R.R. (1985). Effect of the vesicular stomatitis-virus matrix protein on the lateral organization of lipid bilayers containing phosphatidylglycerol – use of fluorescent phospholipid analogs. *Biochemistry* **24**, 7651–7658.
21. Yechiel, E. & Edidin, M. (1987). Micrometer-scale domains in fibroblast plasma membranes. *J. Cell Biol.* **105**, 755–760.
22. Jones, M.E. & Lentz, B.R. (1986). Phospholipid lateral organization in synthetic membranes as monitored by pyrene-labeled phospholipids: effects of temperature and prothrombin fragment-1 binding. *Biochemistry* **25**, 567–574.
23. Friere, E., Markello, T., Rigell, C. & Holloway, P.W. (1983). Calorimetric and fluorescence characterization of interactions between cytochrome-*b*5 and phosphatidylcholine bilayers. *Biochemistry* **22**, 1675–1680.
24. Galla, H.-J. & Sackmann, E. (1974). Lateral diffusion in the hydrophobic region of membranes: use of pyrene excimers as optical probes. *Biochim. Biophys. Acta.* **339**, 103–115.
25. Galla, H.-J. & Sackmann, E. (1975). Chemically induced phase separation in mixed vesicles containing phosphatidic acid. An optical study. *J. Amer. Chem. Soc.* **97**, 4114–4120.
26. Mallik, S., *et al.*, & Arnold, F.H. (1994). Towards materials for the specific recognition and separation of proteins. *New J. Chem.* **18**, 299–304.
27. Hartmann, W., Galla, H.-J. & Sackmann, E. (1977). Direct evidence of charge-induced domain structure in model membranes. *FEBS Lett.* **78**, 169–172.
28. DeTar, D.F. & Silverstein, R. (1966). Reactions of carbodiimides. I. The mechanisms of the reactions of acetic acid with dicyclohexylcarbodiimide. *J. Amer. Chem. Soc.* **88**, 1013–1019.
29. Losche, M., Sackmann, E. & Mohwald, H. (1983). A fluorescence microscopic study concerning the phase diagram of phospholipids. *Ber. Bunsenges. Phys. Chem.* **87**, 848–852.
30. Peters, R. & Beck, K. (1983). Translational diffusion in phospholipid monolayers measured by fluorescence microphotolysis. *Proc. Natl. Acad. Sci. USA* **80**, 7183–7187.
31. McConnell, H.M., Tamm, L.K., & Weis, R.M. (1984). Periodic structures in lipid monolayer phase transitions. *Proc. Natl. Acad. Sci. USA* **81**, 3249–3253.